CHAPTER 244

Effect of Wave-Induced-Pressure on Seabed Configulation

Tetsuo Sakai[1], M. ASCE and Hitoshi Gotoh[2]

Abstract

In almost all of the previous studies on the seabed configuration, the seabed configuration is classified based on the bottom shear stress, or Shields number. While, in the wave field, the wave-induced-water-pressure change can have a secondary effect on the sediment transport. The laboratory experiment on the seabed configuration under the coexistence of the oscillatory flow and the water-pressure change is conducted in this study, to investigate the effect of water-pressure change on the seabed regime classification.

The existing region of various bed configurations, such as no-motion, bed-lad, suspension over ripple and sheet flow, changes with the change of the amplitude of water-pressure change. The ripple geometry, or flatness of ripple, are also affected by the water-pressure change. The mechanism of theses changes are discussed related to the lift force due to the porewater-pressure distribution in sand layer.

Introduction

Seabed configuration, which is formed as the result of sediment transport, is quite different under the various conditions of wave and current. On the other hand, the mode of sediment transport depends on the seabed configuration.

Although there is an interactive structure among the wave-current field, the sediment transport and the seabed configuration, the time scale of the development of seabed configuration is sufficiently longer than that of others. Therefore, to describe

---

[1] Professor, Department of Civil Engineering., Kyoto University
Yoshida Honmachi, Sakyo-ku, Kyoto, 606, Japan
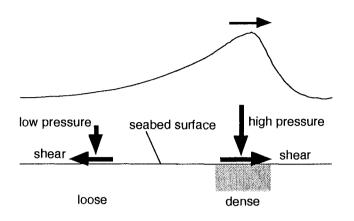[2] Lecturer, Department of Civil Engineering., Kyoto University

Figure 1.   Forces acting on seabed under the wave propagation

the sediment transport process based on the mechanics of the motion of sediment particles, it is essential to know the relation between the seabed configuration and the bottom shear stress, or Shields number, due to wave and current.

These relation has been investigated through some experimental studies; while the effect of wave-induced-water-pressure change on the seabed configuration was not examined in detail.   Fig. 1 shows the schematic expression of external forces acting on seabed due to the wave propagation.   High water pressure acts on the seabed under the crest of a wave, then the particle density of the bed becomes to be dense.   On the other hand, low water pressure acts on the seabed under the trough of a wave, then the particle density of the bed becomes to be loose.   In both situations, the bottom shear stress is the dominant driving force of sediment motion.   To discuss the additional effect due to the water-pressure change by wave propagation in detail, porewater pressure distribution should be investigated.

In this study, the experiment on the seabed configuration under the coexistence of the oscillatory flow and the water-pressure change is performed by using an oscillating water tunnel with cylinder system for the control of the water pressure.

Laboratory experiment

experimental apparatus

Figure 2 shows the oscillating water tunnel with the water-pressure-control system. Both sides of the rectangular water tank are connected to the water circulating pipe, at the top of which a water-circulating-propeller system, or an oscillatory-flow generator,
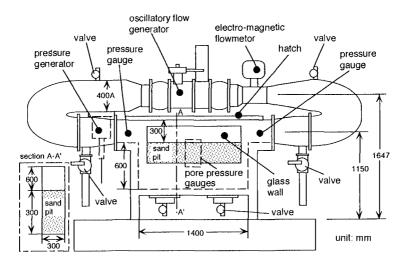
Figure 2. Oscillating water tunnel with water-pressure-changing system

is installed. Lower part of the water tank is a sand pit, the depth of which is 600 mm. The front and back sides of the water tank is made by glass wall for the observation of the motion of sediment particles. In the back side wall, porewater-pressure sensors are flash mounted. In order to generate the water-pressure change, a oil-hydraulic-pressure-driven piston system is connected to the water-circulating pipe. The electromagnetic current meter and the water-pressure sensors are equipped to monitor the discharge of current and the changing water pressure, which are used as the feedback signal of the personal-computer based current-water-pressure control system. Although various kinds of the time series of current-velocity and water-pressure can be generated by using this apparatus, the in-phase sinusoidal time series of current-velocity and water-pressure, which correspond to the condition of a progressive small amplitude wave, are generated.

procedure of experiment and experimental conditions

The transition of bed configuration occurs with the increase of the bottom shear stress in the following order: (i) no motion; [critical state for sediment movement]; (ii) bed-load motion; (iii) suspended load over ripples; and sediment transport in sheetflow regime. In the experiment, the flow-velocity amplitude is gradually increased with keeping the amplitude of water-pressure change, to observe the transition of bottom

Table 1.   Experimental conditions

	oscillatory flow	oscillatory flow and pressure
velocity amplitude u_b (cm/s)	3.0 - 78.0	3.0 - 78.0
total pressure amplitude p_0 (m)	0.0	0.5, 1.0, 1.5
period T (s)	6.0	6.0

configuration mentioned above.   The series of the experiment were conducted with changing the magnitude of the amplitude of the water-pressure change, to investigate the effect of the water-pressure change on the transition of the bed configuration.

The ripple geometry affected by the amplitude of water-pressure change is examined based on the detailed observation of sediment motion over ripples, and the mechanism to determine the ripple geometry is considered.

Table 1 shows the experimental conditions.   The test particle are the two kinds of the uniform sand, the diameter of which are $d=0.025$ cm and $d=0.035$ cm.   The specific density of the sand is 2.65.

Classification of the seabed configuration

Figure 3 shows the experimental results of the bed configuration under the action of oscillatory flow for the cases of $d=0.025$ cm and $d=0.035$ cm.   The lines in this figure shows the division of the bed configuration proposed by Shibayama and Horikawa (1982).   In the figure, u_b=amplitude of the flow velocity in the neibourhood of the bottom; w=terminal fall velocity of sediment particle; and Ψ=Shields number defined as $\psi = f_w u_b^2 / 2(\sigma/\rho - 1)gd$ (f_w=friction coefficient proposed by Jonsson (1966); σ=density of sediment; ρ= density of water; and g=graviational acceleration).   The flow velocity in the neighborhood of the bottom is estimated by extrapolating the measured velocity near-bottom-wall region by supposing the logarithmic velocity profile. The friction coefficient was calculated by using the explicit expression proposed by Tanaka (1990).   The thresholds of four modes, such as no motion, bed-load motion, suspension over ripples and sheetfolw, estimated from the present experiment show fairly good agreement with the empirical relation proposed by Shibayama and Horikawa, which was determined based on the existing experimental results.
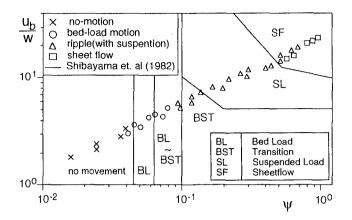
Figure 3.   Classification of seabed

Figure 4 shows the classification of the bed configuration, namely, no motion, bed-load, suspension over ripple and sheetflow, under the various combination of flow-velocity amplitude, u_b, and total water-pressure-change amplitude, p. In this figure, the experimental results of the cases of the particle diameter $d=0.025$ cm are shown. The critical shear stress of the sediment movement decreses with the increase of the amplitude of water-pressure change. In other words, the no-motion region decrease with the increase of the amplitude of water-pressure change. The supression of the ripple generation increases with the increase of the amplitude of water-pressure change, consequently, the be-load region increase with the increase of the amplitude of water-pressure change. In contrast with the ripple genaration, the generation of the sheetflow is promoted by the increase of the amplitude of water-pressure change.

The changing porewater pressure is induced in the sandy bed constituted by fine sediment under the action of water-pressure change on the bed surface. Because of the phase lag between the porewater pressure and the water-pressure acting on the sand surface, an additional lift force acts on the sediment layer near the sand surface. This additional lift force depends on the porewater-pressure profile, and the positive lift force acts on the sediment layer when the changing water-pressure is smaller than the average, namely in wave-trough phase. The decrease of the critical bottom shear stress of sediment movement is caused by the action of this additional lift force.

Figure 5 shows the classification of the bed configuration under the various combination of flow-velocity amplitude, u_b, and water-pressure-change amplitude, p,
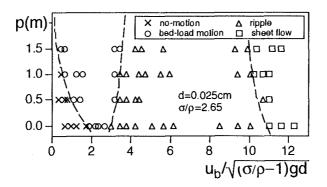
Figure 4.   Classification of the bed configuration ($d=0.025$ cm)
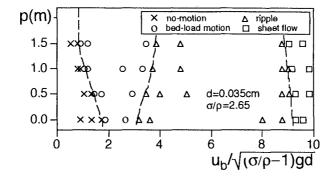

Figure 5.   Classification of the bed configuration ($d=0.035$ cm)

for the particle diameter $d=0.035$ cm.   Although the tendency of the transition of bed configuration shown in Fig. 5 is the same as in Fig. 4, the effect of the amplitude of the water-pressure change to the transition of the bed configuration is stronger in Fig. 4 than that in Fig. 5.   To clarify this point, the bottom neighboring flow velocities, u_{cp}, at three threshold such as the transition point from no motion to bed load, from bed-load to suspension and from suspension to sheetflow for the change of the amplitude of water-pressure change are shown in Fig. 6.   The bottom neighboring flow velocities, u_{cp}, are normalized by that of oscillatory flow condition, u_c.   Fig. 6 shows that the transition points of the bed configuration clearly depend on the magnitude of the
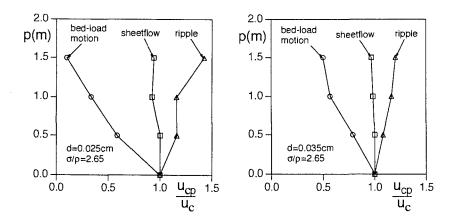
Figure 6.   Transition points of the bed configuration

amplitude of water-pressure change.   This tendency is most clearly detected in the transition point from no motion to bed load.   By comparing the cases of d=0.025 cm and the cases of d=0.035 cm, the change of the threshold of bed configuration against the change of the amplitude of water-pressure change in small size sediment is more significant than that in large size sediment.

Under the action of critical bottom shear stress of sediment movement, hydrodynaminc force, or driving force, acting on the sediment particle balances with the bottom frictional force, or resistant force.   Therefore the sediment motion is keenly affected by the additional lift force due to the changing porewater pressure in sand layer.   While, in the cases of the transition from suspension to sheetflow, the amplitude of the bottom shear stress are sufficiently larger than that of no-motion-bed-load transition.   Hence the bottom shear stress plays a significant role in the transition from suspension to sheetflow, and the change of the threshold from suspension to sheetflow against the change of the water-pressure amplitude is smaller than that from no motion to bed load.

Geometry of ripples under coexistence of shear and water-pressure changes

The geometry of ripples in suspension mode is also affected by the change of the amplitude of water-pressure change.   Maeno et al. (1989) conducted the experiment on the ripple geometry under the action of porewater pressure in sandy bed.   They mainly discussed the energy dissipation due to the ripples based on the measurement of the porewater pressure change.   While in this study, the role of the porewater pressure
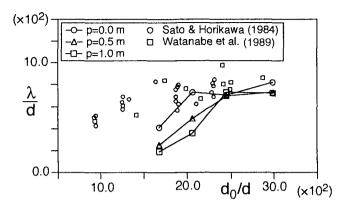
Figure 7.   Relation between ripple wave length and excursion length
              of water particle

change in sandy bed is investigated as a part of the mechanism to determine the ripple
geometry.

Figure 7 shows the relation between ripple wave length, λ, and excursion length
of water particle, d_0.   In this figure, the cases of three kinds of total water-pressure
amplitude, p=0.0, 0.5 and 1.0 m are shown with the experimental result by Sato et al.
(1984) and Watanabe et al. (1989).   In the region of $15.0<d_0/d<25.0$, the ripple wave
length decreases with the increase of amplitude of water-pressure change; while, in the
region of $25.0<d_0/d$, the dependence of ripple wave length on the amplitude of water-
pressure change becomes less significant, and the ripple wave length is regarded to be
constant.

Figure 8 shows the relation between ripple wave steepness, η/λ, and Shields
number, Ψ (η=ripple wave height) .   In this figure, the cases of three kinds of total
water-pressure amplitude, p=0.0, 0.5 and 1.0 m are shown with the experimental result
by Sato et al. (1984) and Watanabe et al. (1989).   In the region of small Shields
number, or in the region of ripple generation, the ripple wave length decreases with
the increase of amplitude of water-pressure change.   In other words, ripples become
flatter with the increase of amplitude of water-pressure change.   This tendency becomes
less significant with the increase of Shields number.   In the neighborhood of Ψ=0.3,
the dependence of the ripple wave length on the amplitude of water-pressure change is
not clear.

Figure 9 shows the change of the transition from two-dimensional ripples to
three-dimensional ripples with the change of the amplitude of water-pressure change.
The dashed lines in this figure shows the threshold of two- and three-dimensional
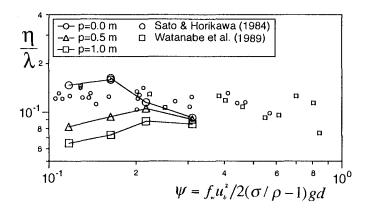
Figure 8. Relation between ripple wave steepness and Shields number

ripples proposed by Watanabe et al. (1989). In the pure oscillatory cases, $p=0.0$ m, the experimental results agree fairly well with the proposal by Watanabe et al. The transition point from two-dimensional ripple to three-dimensional one gradually decreases with the increase of d_0/d. In the coexistence cases of oscillatory flow and water-pressure change, the transition point from two-dimensional ripple to three-dimensional one shifts upward, and the dependence of the transition point to the excursion length of water particle becomes smaller.

Two-dimensional ripples are dominantly observed when the ripple wave length and the ripple wave steepness is affected by water-pressure change. The motion of sediment in the neighborhood of the crest of ripple was recorded by a CCD video camera, to investigate the flatting process of ripple due to the water-pressure change in detail. Table 2 shows the experimental condition. Figure 10 shows the behavior of sediment at every $3/\pi$ intervals on the symmetric ripple, which is generated in the pure oscillatory flow condition, $p=0.0$ m. On the other hand, Fig. 11 shows the behavior of sediment on the asymmetric ripple, which is generated in the oscillatory flow and water-pressure change coexisting condition ($p=1.0$ m).

For the simplicity, direction of the current form left to right is taken positive, and the opposit one is taken negative. In this study, the oscillating flow is in phase with the water-pressure change, hence the pressure differnce from the average is positive when the current direction is positive; while the pressure difference from the average is negative when the current direction is negative.

In the pure oscillatory flow case, the time series of the current velocity follows the sinusoidal curve, then the flow velocity is symmetric between the positive-current phase and negative-current phase. Two ripple geometry with the phase lag π are
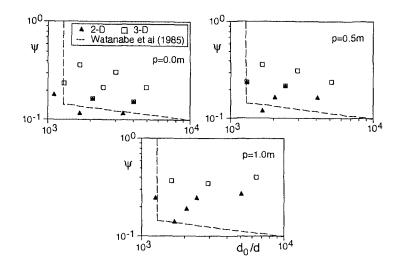
Figure 9. Transition from two-dimensional ripples to three-dimensional ripples

Table 2. Experimental conditions of the visualization

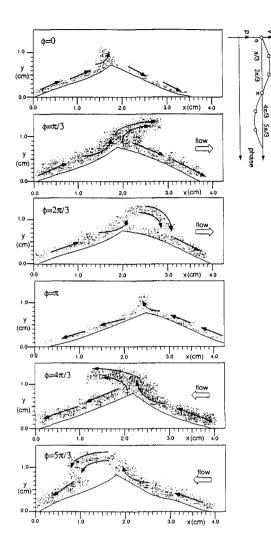|	oscillatory flow	oscillatory flow and pressure
velocity amplitude u_b (cm/s)	29.0	29.0
total pressure amplitude p_0 (m)	0.0	1.0
period T (s)	6.0	6.0
diameter of sand d(cm)	0.025	
specific density of sand σ/ρ	2.65	
ripple wave length λ(cm)	20.0	23.0
ripple wave height η(cm)	2.5	2.0

Figure 10. Behavior of sediment at every $3/\pi$ intervals on the symmetric ripple

symmetric. On the contrary, under the coexistence of oscillatory flow and water-pressure change, a significant asymmetric ripple geometry is detected between the positive-current phase and the negative-current phase. Suspended sediment transported along a backward slope of the ripple in the negative-current direction at the phase $\phi=4\pi/3$ is significantly larger than that in the positive-current direction at the phase
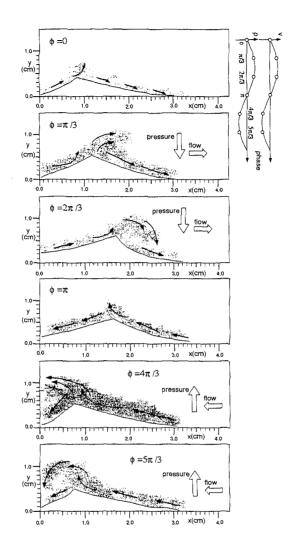
Figure 11. Behavior of sediment at every $3/\pi$ intervals on the asymmetric ripple

$\phi=\pi/3$.   When the pressure difference from the average is negative, or the current direction is negative, the additional lift force due to the porewater pressure in sand layer acts on the sediment particles near the surface of sand layer.   Because of this additional lift force, sediment particles are promoted to be dislodged, consequently the sediment transport rate increases.   On the other hand, when the pressure difference
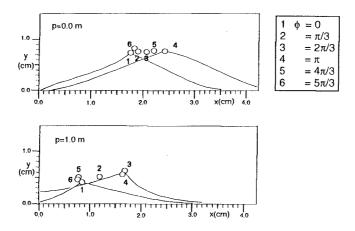
Figure 12. Movement of the crest of ripple

from the average is positive, or the current direction is positive, the negative lift force, or the additional force acting in downward direction, due to the porewater pressure in sand layer acts on the sediment particles near the surface of sand layer. This force increases the resistance of the sediment particle against the dislodgment and, consequently the sediment transport rate decreases.

Figure 12 shows the movement of the crest of ripple during one oscillating cycle. In the symmetric ripple, which is generated under the pure oscillating flow (p=0.0 m), the moving path of the crest toward right and that toward left overlap with each other. In other word, the vertical displacement of the crest of ripple is sufficiently small compared with the horizontal motion of the crest of ripple. On the contrary, in the case of the coexistence of the oscillatory flow and water-pressure change, the moving path of the crest during the positive-current-direction phase and that during the negative-current direction phase is significantly different. The moving velocity of the crest is slower during the positive-current-direction phase (1-3 in Fig. 12) than during the negative-current-direction phase (4-6 in Fig. 12). The crest of ripple moves upward during the positive-current-direction phase and moves downward during the negative-current-direction phase. Because the ripple wave length is approximately constant in all phases, this characteristics of the ripple wave height, or the movement of the crest in vertical direction, are interpreted as the change of the ripple wave steepness. The ripple wave steepness is larger during the positive-current-direction phase than during the negative-current-direction phase. The additional force due to porewater pressure induced by water-pressure change acts in upward direction during the negative-current-direction phase. This additional force brings the decrease in the apparent angle of

repose of sand, and the resultant flatting of ripple geometry.

Conclusion

In this study, the experiment on the seabed configuration under the coexistence of the oscillatory flow and the water-pressure change is performed by the oscillating water tunnel with cylinder system for the control of the water pressure.

The existing region of various bed configurations, such as no-motion flat bed mode, bed-load mode, suspension over ripple bed and sheet flow, changes with the change of the amplitude of water-pressure change. Furthermore, the ripple geometry, such as ripple wave length and wave steepness, or flatness of ripple, are also affected by the amplitude of water-pressure change.

Lift force due to the porewater-pressure distribution in sand layer acts in both upward and downward direction. The upward lift force promotes a sediment motion; while the downward force, or negative lift force, suppress a sediment motion. These difference of the sediment motion is the reason of the change of the existing region of the dominant bed configuration and the asymmetric characteristics of ripple geometry.

References

Jonsson, I. G.(1966): Wave boundary layer and friction factors, Proc. of 10th Conf. on Coastal Eng., pp.127-148.

Maeno, Y, Matsuoka, Y, Hayashida, H. and Mase, H.(1989): Effects of ripple geometry on wave-induced pore pressure, Proc. of Coastal Eng., JSCE, Vol. 36, pp. 789-793(in Japanese).

Sato, S. and Horikawa, K.(1984): Laboratory study on sand transport over ripples due to asymmetrical oscillatory flows, Proc. of Coastal Eng., JSCE, Vol. 31, pp. 286-290(in Japanese).

Shibayama, T. and Horikawa, K.(1982): Sediment transport and beach transformation, Proc. 18th ICCE, pp.1439-1458.

Tanaka, H.(1990): An explicit expression of a friction coefficient for a wave-current coexisting motion, Proc. of JSCE, No. 417/II-13, 285-288 (in Japanese).

Watanabe, A., Sakinada, M. and Isobe, M.(1989): Ripple formation and sand transport rate in a wave-current coexistent system, Proc. of Coastal Eng., JSCE, Vol. 36, pp. 299-303(in Japanese).